

In-silico model of the pregnant uterus as a network of oscillators under sparse adaptive control

Giuseppe M. Ferro¹, Andrea Somazzi², and Didier Sornette³

¹Department of Ecology and Evolutionary Biology, Princeton University, Princeton, NJ 08544

²IMT School for Advanced Studies, Piazza S. Francesco 19, 55100 Lucca, Italy

³Institute of Risk Analysis, Prediction and Management (Risks-X) Southern University of Science and Technology (SUSTech) Shenzhen, 518055, China

July 2024

Abstract

To ensure optimal survival of the neonate, the biological timing of parturition must be tightly controlled. Medical studies show that a variety of endocrine systems play the role of a control system, establishing a dynamic balance between the forces that cause uterine quiescence during pregnancy and the forces that produce coordinated uterine contractility at parturition. These control mechanism, and the factors that affect their performance, are still poorly understood. To help fill this gap, we propose a model of the pregnant uterus as a network of FitzHugh-Nagumo oscillators, with each cell symbolizing the electrical activity of a myocyte. The model is augmented with sparse adaptive control mechanisms representing the regulating endocrine functions. The control system is characterized by the fraction of controlled sites, and strength of control. We quantitatively find the conditions for which the control system exhibit a balance between robustness (resilience against perturbations) and flexibility (ability to switch function with minimal cost) crucial for optimal neonatal survival. Specifically, we show that Braxton-Hicks and Alvarez contractions, which are observed sporadic contractions of the uterine muscle, serve as a safety valve against over-controlling, strategically suppressed yet retained to optimize the control system's efficiency. Preterm birth is suggested to be understood as a mis-identification of the control boundaries. These insights contribute to advancing our understanding of maternal-fetal health.

1 Introduction

In biological systems, the balance between robustness and flexibility is crucial for ensuring both stability and adaptability [1]. Robustness refers to a system's ability to consistently perform a specific function under varying and uncontrolled conditions, while flexibility is the ability to adapt and change function as conditions shift.

Such balance is also evident in the context of parturition. As described in [2, 3], the control of pregnancy — with its many autocrine, paracrine and mechanical influences — creates a dynamic equilibrium between the forces that maintain uterine quiescence and those that promote coordinated uterine contractions. Such balance satisfies the need to maintain a stable pregnancy despite exogenous perturbations, while ensuring a timely initiation of labor. The uterus, which can exhibit synchronized contractions early in pregnancy [4], is kept quiescent by an elaborate control system that prevents myocytes from contracting and synchronizing. This explains the abrupt transition from a stable pregnancy to labor within a few hours, showcasing the coexistence of robustness (structural stability and minimal fine-tuning of control parameters) and flexibility (ability to switch function with minimal effort).

Several mathematical models of parturition have been proposed. One class of models [5, 6] focuses on the progressive synchronization of uterine cells, describing parturition as a critical phase transition. A critical bifurcation would predict increasing susceptibility and variance as term approaches, which is incompatible with being robust against perturbations. Another class of models [7, 8] does an excellent job in characterizing the electro-chemical-mechanical properties of uterus and cervix. However, the above mentioned control aspect of pregnancy is often overlooked.

In this paper, we build on the concept of pregnancy as a control system, extending an existing model of the uterus to explicitly account for the action of a biologically thrifty control that suppresses oscillations. As a result of a cost-effective control strategy, our model predicts the occurrence of empirically observed different types of pre-labor contractions, such as Alvarez waves and Braxton-Hicks contractions [9], which we interpret as occasional malfunctions of the control system.

By incorporating the balance between robustness and flexibility into our model, we aim to provide a more comprehensive understanding of the dynamics of parturition, which could lead to better understanding of pre-term births, experienced in over 10% of pregnancies, accounting for more than a third of all infant deaths [10, 11].

In Section 2 we introduce the model. Section 3 summarizes the main results (SI complements). We discuss broader implication of the model in Section 4. Section 5 concludes.

2 Methods

Our point of departure is the model in [6]. They model the uterine tissue as a two-dimensional medium $L \times L$ of excitable cells (uterine myocytes) and electrically passive cells (fibroblasts and interstitial Cajal-ike cells). $L = 32$ throughout the paper. In isolation, each excitable cell is connected to n_p passive cells. The electrical activity of a myocyte and one or more passive cells is described by the following system of ordinary differential equations:

$$\begin{aligned}\frac{dV_e}{dt} &= AV_e(V_e - \eta)(1 - V_e) - g + n_p C_r(V_p - V_e) \\ \frac{dg}{dt} &= \epsilon(V_e - g) \\ \frac{dV_p}{dt} &= K(V_p^R - V_p) - C_r(V_p - V_e)\end{aligned}\tag{1}$$

where V_e and V_p represent the electrical activity of the active cell and n_p identical passive cells. As for parameters characterizing the active cell, g is an effective membrane conductance, η is the excitation threshold, A specifies the activation kinetics, and ϵ dictates the recovery rate of the medium. For the passive cell, V_p^R is the resting state while K characterizes how fast the system relax to V_p^R . The passive cells are assumed to be linearly coupled with the active element with strength C_r . The parameters $A(= 3)$, $\eta(= 0.2)$, $\epsilon(= 0.08)$, $K(= 0.25)$, $V_p^R(= 1.5)$ are fixed as suggested by [6]. Varying the number of passive cells n_p and the passive-active coupling C_r , the cell goes from quiescent to oscillatory behavior through a Hopf-bifurcation.

To explore the emergence of spatial organization in the system, the dynamics of the active cells medium are augmented as follows:

$$\frac{dV_e}{dt} = AV_e(V_e - \alpha)(1 - V_e) - g + n_p C_r(V_p - V_e) + D\nabla^2 V_e\tag{2}$$

where D captures the coupling between excitable elements. Passive cells are not coupled to each other and only coupled to myocytes. ∇^2 is the discrete Laplace operator. In the extended system, excitable cells are thus connected to each other. Excitable cells are also linked to n_p passive cells, with n_p following a Poisson distribution characterized by a mean value f . Consequently, f is an indicator of the passive cell density in relation to the myocytes. Synchronized activity emerges through coupling, increasing D leads to: i) increased correlation between elements; ii) more and more elements oscillate with the same frequency.

We imagine that a fraction n_c of the cells composing the uterus is kept inactive by an adaptive control μ , evolving in time to suppress oscillations. The first equation of the system (2) is then rewritten as

$$\frac{dV_e}{dt} = AV_e(V_e - \eta)(1 - V_e) - g + n_p C_r(V_p - V_e) + D\nabla^2 V_e - \mu,\tag{3}$$

where $\mu(t) = 0 \forall t > 0$ if the considered cell is among those which are not controlled. Otherwise, the control $\mu(t)$ evolves in time trying to lead the cell's voltage to a target value V_T and to keep it constant. The control measures the cell's voltage and uses it to update itself, with a delay τ . This process translates into the differential equation:

$$\frac{d\mu}{dt} = \gamma(\alpha r(t - \tau) - \mu), \quad (4)$$

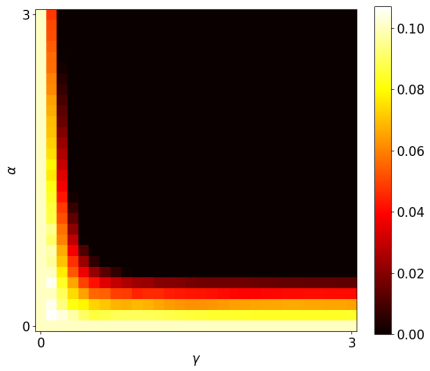
where $r = V_e(t - \tau) - V_T$ is the difference between the measured and target cell's voltage. The presence of the minus μ term in the r.h.s. of the equation represents the self regulation of the control, which otherwise could potentially become unrealistically (from a biological perspective) large. The trade-off between suppression of oscillation and cost of control is captured by the parameter $\alpha \geq 0$. The control evolves with a time-scale $\frac{1}{\gamma}$.

We have simulated the equations with a fourth-order Runge-Kutta algorithm, with a time step of $dt = 0.1$, for 2^{15} time units.

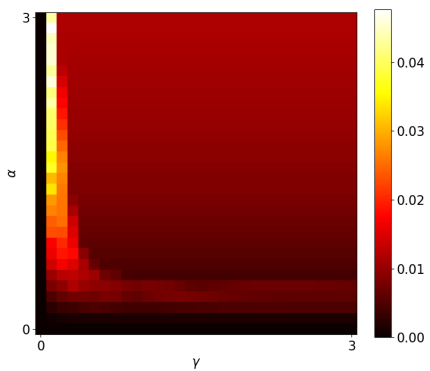
3 Results

3.1 Single cell control ($D = 0$)

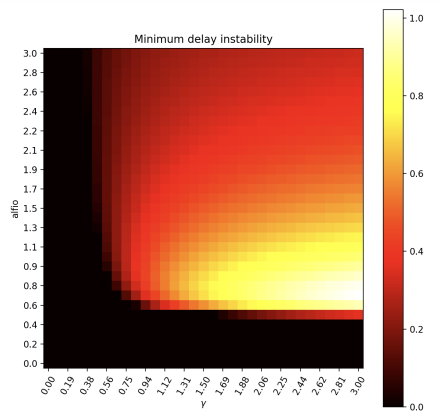
Let us start from one active cell (1) in presence of control (4). In absence of control, $C_r (= 1)$ and $n_p (= 1)$ are set so that the cell would spontaneously oscillate. To characterize the effectiveness of the control, we compare the asymptotic power of the signal minus its average $\frac{1}{T - T_{eq}} \int_{T - T_{eq}}^T (V_e - \bar{V}_e)^2(t) dt$ — as a proxy for oscillation — vs the asymptotic control effort, measured as $\frac{1}{T - T_{eq}} \int_{T - T_{eq}}^T \mu^2(t) dt$.



(a)



(b)



(c)

Figure 1: For different values of γ and α , we show: (a) the power of the signal for $\tau = 0$; (b) the control effort for $\tau = 0$; (c) the minimum value of delay τ that would lead to oscillatory behavior. $n_p = C_r = 1$.

The performance of the control should be understood in the context of possible perturbations to its parameters, α , γ and τ . Ideally, the control should strive for a trade-off between robustness and flexibility: while external perturbations of the parameters should not cause abrupt and undesired change of state, the body has to keep the ability to efficiently switch function. In Figure 1, we show the γ - α phase diagram for a single controlled cell. When $\tau = 0$, there is an hyperbola-like curve which separates the phase space into an oscillatory and a quiescent region. Since the control's effort is roughly constant in the quiescent region (see Fig. 1b), every couple (γ, α) in that region is equally good from an energetic perspective, showing considerable robustness. However, when also considering a finite delay τ , it becomes imperative for the control to have parameters' values which allow the system to be stable (see Fig. 1c). As shown in the supplementary material, the γ - α phase diagram is almost identical when changing values of C_r and n_p , showing an additional dimension of robustness.

3.2 Control of distributed system

Having discussed the one cell control, we now turn our attention to the spatially extended system (Eqs. 3 and 4). We place ourselves in the *global synchronization* regime, where, without control, all elements in the medium oscillate at the same frequency, with a single wave traversing the entire system (see Fig. 2b). We choose $D = 1$, $C_r = 1$ and passive cell density $f = 0.7$. Looking at Eq. 4, in principle, each site (i, j) can have its own control parameters γ_{ij}, τ_{ij} and α_{ij} . If the objective of the control is to suppress oscillations while minimizing control effort, we suppose that each combination of α_{ij} represents a control strategy in the action space, while γ and τ embody physical constraints. For simplicity, we set the time-scale $\gamma = 1$ and the delay $\tau = 0$ to be homogeneous in the medium (in the SI we explore different physical constraints). As for the α_{ij} , to reduce the dimensionality of the strategy space, we assume them to be i.i.d according to the following bimodal distribution:

$$\rho(\alpha_{ij}) = n_c \delta(\alpha_{ij} - \alpha) + (1 - n_c) \delta(\alpha_{ij}) \quad (5)$$

Eq. 5 amounts to have a fraction n_c of controlled sites with parameter α . Similarly to the single cell case (Section 3.1), we characterize the control performance by the fraction of oscillating sites f_o and asymptotic control effort

$$\begin{aligned} f_o &= \frac{1}{L^2} \sum_{i,j} H(p_{ij} - p_{th}) \\ \bar{\mu} &= \frac{1}{L^2} \sum_{i,j} \left(\frac{1}{T - T_{eq}} \int_{T - T_{eq}}^T dt \mu_{ij}^2(t) \right) \end{aligned} \quad (6)$$

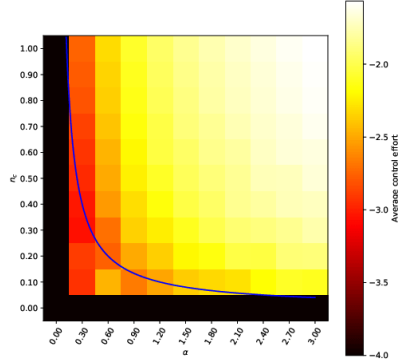
where p_{ij} is the power of cell ij , p_{th} is a threshold value and $H(x)$ is the heavy-side function. Clearly, $\mu_{ij}(t) = 0 \forall t$ if the site is not controlled. Fig. 2a shows a heatmap of the control effort in the $n_c - \alpha$ plane, together with the line separating two phases: a controlled region — $f_o = 0$ — and a non-controlled

one with $f_o > 0^1$. Note that the transition is continuous, with f_o gradually going to 0 (see Figs. 2c and 2d). The line separating the regions is of the form $n_c \alpha = k$, where the specific value of k depends on the coupling D between cells (see SI).

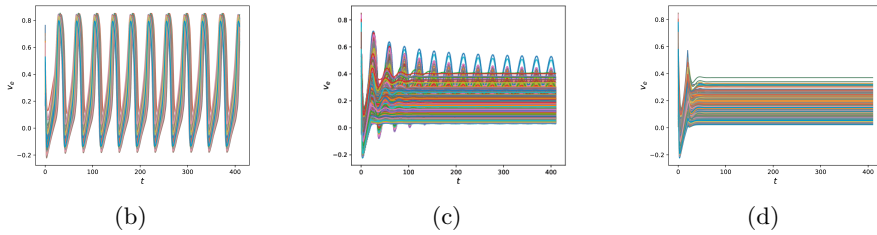
Intuitively, for $D = 0$, every cell would need to be controlled to suppress all oscillations, while higher values of D allow a sparse control to be as effective. As expected, the control effort is increasing both in n_c and α , but, surprisingly, a strategy with high n_c and low α is less costly than a strategy with low n_c and high α . As already mentioned in Section 3.1, the control plausibly aims for a trade-off between robustness, flexibility and effort. Depending on the exact characterization of this trade-off, the optimal strategy is in the vicinity of the phase transition²[1]. In the next section we explore the behavior of the system when subjected to structural perturbations.

¹The phase transition in Fig. 2b is robust to changes in p_{th} across different orders of magnitude.

²Following the control theory literature [12], one could construct a cost function that compares the amount of oscillations with the control effort. A simpler route is to assume a two-step optimization process. The control prioritizes the suppression of oscillations and then, conditional on this, minimizes the effort.



(a)



(b)

(c)

(d)

Figure 2: Sparse control in the global synchronization regime. (a) Heatmap of control effort (logarithmic scale) in the $n_c - \alpha$ plane together with phase transition line ; (b) uncontrolled situation ($f_o = 1$) ; (c) ‘almost’ controlled ($f_o \simeq 0$); (d) fully controlled ($f_o = 0$).

3.3 Response to perturbations

In this section, we explore the consequences of the above mentioned trade-off between robustness, flexibility and effort in response to structural perturbations. Suppose that the control is operating with a given n_c and α . We imagine that perturbations manifest in the form of fluctuations of the parameter α .

For a given n_c , denote by C the set of controlled sites. The fluctuations are described by the following stochastic differential equation

$$d\alpha_i = \theta(\alpha - \alpha_i)dt + \sigma dW_t^i, i \in C \quad (7)$$

Eq. 7 describes an Ornstein-Uhlenbeck process, with θ and σ impacting the mean reversion rate and standard deviation of the process — and W_t^i is a standard Wiener process. We consider the case of uncorrelated Gaussian increments

across time and space

$$\langle dW_t^l dW_t^k \rangle = \delta_{lk} \delta(t - t') \quad (8)$$

This describe a situation where each site independently experiences perturbations. In the SI, we explore also the scenario where the perturbations are fully correlated in space but uncorrelated in time, corresponding to a system-wide perturbation.

We aim to quantify the resulting oscillations caused by the parameter perturbation, depending on the initial $n_c - \alpha$ point. We investigate the set of points specified by $n_c \alpha = k' > k$. These strategy subset ensures $f_o = 0$ in absence of perturbations and all of them have the same average α . For these comparison to be meaningful, we imagine to keep constant the relative precision at each α value. Therefore, $\sigma(\alpha)$ is such that the coefficient of variation $\frac{\Delta\alpha}{\alpha}$ for each α is constant. Fig. 3a shows the average power per site along the $n_c \alpha = k'$ strategy points. The strategy with high n_c and low α appears to be the most robust to perturbations, while being the most cost effective at the same time (see Fig. 2b). This is intuitively reasonable, as the probability that $n_c L^2$ sites jointly experience a negative perturbation is lower for high n_c .

However, such a pervasive control might not be feasible (see Section 4). Let us therefore better characterize the nature of these oscillations when the high n_c low α strategy is not available. Denoting with x the spatial ‘size’ of a given oscillation, in Figure 3b, we plot the empirical complementary cumulative distribution function $P(X > x)$ for $n_c = 0.3$ and $\alpha = 0.9$ and $\frac{\Delta\alpha}{\alpha} = 0.5$. The distribution resembles a (truncated) power-law, with the exponent being determined by the coefficient of variation and the control strategy. Even with uncorrelated perturbation, the model predicts localized waves as well coherent ones — with non negligible probability — that traverse a significant part of the medium. Fig. 3c shows, for each given wave size, the average power per size. The upward trend reveals that the more localized waves have smaller amplitude, in agreement with empirical observations (see Section 4). Finally, in Fig. 3d we plot a typical voltage profile of a given site, showing the superposition of high frequency low amplitude waves and low frequency high amplitude ones, again qualitatively agreeing with empirical data [9].

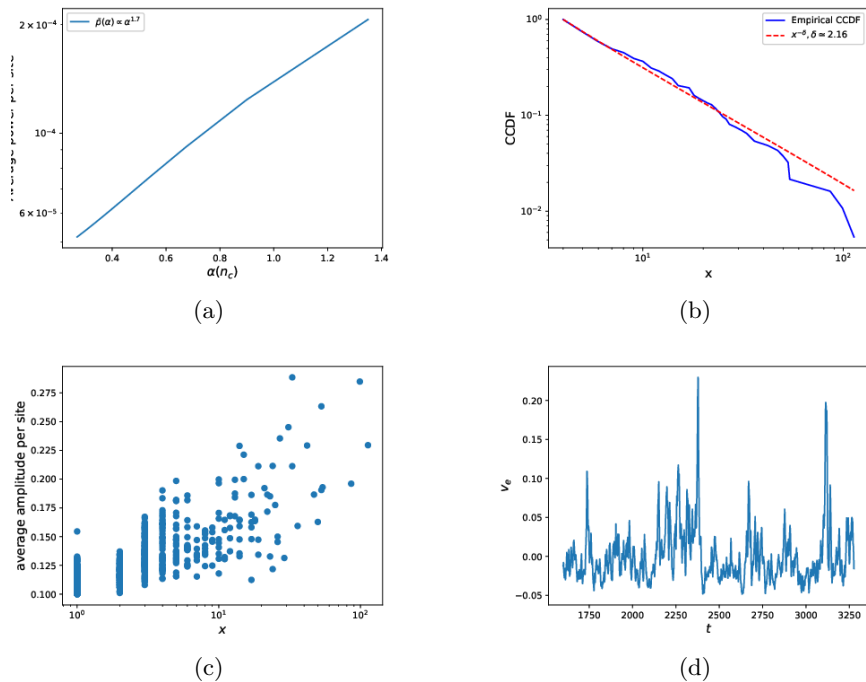


Figure 3: (a) Average power per site along a subset of $n_c - \alpha$ points. (b) Distribution of wave sizes ; (c) Average power per site as a function of corresponding wave size ; (d) An example of oscillations . Subplots (b)-(c)-(d) are with $n_c = 0.3$, $\alpha = 0.9$ and $\frac{\Delta\alpha}{\alpha} = 0.5$.

4 Discussion

The proposed model describes the uterine change of state from quiescence to labor as driven by the evolution of the parameters D and α . As explained in [6], in the absence of control, increasing D (which represents the formation and strengthening of gap junctions) leads the uterine cells to synchronize. However, as already explained, the divergence of susceptibility and variance implied by a critical transition is incompatible with the necessity for such biological system to be robust to perturbations.

The introduction of a control center — which has the purpose to suppress oscillations before delivery — allows the essential dynamical balance between quiescence and contraction. Through the lens of our model, the control becomes active before D is large enough to cause synchronous oscillations, and it is ‘turned off’ when delivery has to occur. That is a simplified representation of different mechanisms, such as transition from progesterone to estrogen dominance, heightened sensitivity to oxytocin, formation of gap junctions, elevated prostaglandin activity, reduced nitric oxide (NO) activity and increased

calcium influx into myocytes [2]. Such mechanisms keep the uterus resilient to external perturbations, effectively avoiding that the system crosses the critical phase transition as D increases. With respect to Fig 2a, given a certain n_c , α is set at the right of the critical line when D is still small. This ensures that the system never exhibits global synchronization when the control is active.

How the control chooses α among those ensuring quiescence is assumed to be related to its cost effectiveness and the necessity for flexibility, which are predicted to be positively correlated. As a result, it can be surmised that the system is not ‘over-controlled’, and α is set not too far from the critical line, where the control effort is minimal. With respect to the fraction of controlled sites n_c , although we have considered it to be a ‘control variable’, it is reasonable to expect that it can not be tuned arbitrarily, but it is rather a biological — possibly idiosyncratic — constraint. While an high value of n_c corresponds to a smaller cost, it could be very difficult to maintain such a pervasive control. Also, assuming that for a given n_c the control chooses an $\alpha(n_c)$ relatively close to the critical line for energy saving, if $n_c \approx 1$, then α is small and thus the control is less resilient to space-correlated perturbations (see SI).

Our model also predicts the occurrence of contractions happening before delivery. Clustering of EHG recordings [9] essentially finds two types of pre-labor contractions: Alvarez waves (localized, low amplitude and high frequency) and Braxston-Hicks waves (more spread, higher amplitude and lower frequency). Note that the relationship between Alvarez waves, Braxston-Hicks waves and pre-term labor is not clear [4].

As shown in Fig 3b and 3c, our model agrees qualitatively with such observations. Moreover, it predicts a power law distribution of wave size which, depending on increasing data resolution, can be tested. The distribution of such waves can be modulated in various ways. First, one can consider different variances in the OU process in relation to the mean values of α . Also, one can consider a non-trivial correlation matrix among the different stochastic processes. While we have shown uncorrelated random processes, it is possible to consider a correlation matrix taking into account, for example, spatial proximity. The other limiting case is when the OU processes are fully correlated, meaning that each $\alpha_{ij}(t)$ is equal to the others $\forall t$. This would obviously lead to a larger number of global waves, since a large fluctuation of the OU process would result in *all* the cells becoming effectively uncontrolled for a certain time window.

Considering the broader implications, while our model does not explicitly address preterm birth, it offers insights into potential precursors of this issue. A mismatch between the parameters D and α , such as an error or a delay in turning on the control, could result in the emergence of early global synchronization leading to delivery. Although we have only heuristically argued that the control chooses α close to the critical line to save energy and resources, a model for the minimization of the cost by the control would potentially shed light on pre-term birth.

5 Conclusions

Our study presents a novel in-silico model of the pregnant uterus, conceptualized as a network of FitzHugh-Nagumo oscillators under sparse adaptive control. This model captures the delicate balance between robustness and flexibility required for maintaining uterine quiescence during pregnancy and initiating coordinated contractions during labor.

Our findings suggest that the uterus employs an adaptive control system to suppress myocyte oscillations and prevent premature synchronization. This control system ensures that the uterus remains quiet until the appropriate time for delivery, balancing energy efficiency and functional readiness. Moreover, our model predicts the occurrence of pre-labor contractions, such as Alvarez waves and Braxton-Hicks contractions. These are interpreted as occasional malfunctions of the control system, which act as safety valves to avoid over-controlling and ensure the system's efficiency.

While our model does not explicitly address preterm birth, it offers insights into potential precursors of this issue, highlighting the need for further research.

References

- [1] Marcelo O Magnasco. Robustness and flexibility of neural function through dynamical criticality. *Entropy*, 24(5):591, 2022.
- [2] Gerson Weiss. Endocrinology of parturition. *The Journal of Clinical Endocrinology & Metabolism*, 85(12):4421–4425, 2000.
- [3] Manuel S Vidal Jr, Ryan CV Lintao, Mary Elise L Severino, Ourlad Alzeus G Tantengco, and Ramkumar Menon. Spontaneous preterm birth: Involvement of multiple feto-maternal tissues and organ systems, differing mechanisms, and pathways. *Frontiers in Endocrinology*, 13:1015622, 2022.
- [4] Sara Russo, Arnaldo Batista, Filipa Esgalhado, Catarina R Palma dos Reis, Fátima Serrano, Valentina Vassilenko, and Manuel Ortigueira. Alvarez waves in pregnancy: a comprehensive review. *Biophysical Reviews*, 13:563–574, 2021.
- [5] Alan P Benson, Richard H Clayton, Arun V Holden, Sanjay Kharche, and Wing C Tong. Endogenous driving and synchronization in cardiac and uterine virtual tissues: bifurcations and local coupling. *Philosophical Transactions of the Royal Society A: Mathematical, Physical and Engineering Sciences*, 364(1842):1313–1327, 2006.
- [6] Rajeev Singh, Jinshan Xu, Nicolas G Garnier, Alain Pumir, and Sitabhra Sinha. Self-organized transition to coherent activity in disordered media. *Physical Review Letters*, 108(6):068102, 2012.
- [7] Shuyang Fang, James McLean, Lei Shi, Joy-Sarah Y Vink, Christine P Hendon, and Kristin M Myers. Anisotropic mechanical properties of the

- human uterus measured by spherical indentation. *Annals of biomedical engineering*, 49:1923–1942, 2021.
- [8] DS Fidalgo, M Borges, MCP Vila Pouca, DA Oliveira, E Malanowska, and KM Myers. On the effect of irregular uterine activity during a vaginal delivery using an electro-chemo-mechanical constitutive model. *Journal of the Mechanical Behavior of Biomedical Materials*, 131:105250, 2022.
- [9] Filipa Esgalhado, Arnaldo G Batista, Helena Mouriño, Sara Russo, Catarina R Palma Dos Reis, Fátima Serrano, Valentina Vassilenko, and Manuel Ortigueira. Uterine contractions clustering based on electrohysterography. *Computers in Biology and Medicine*, 123:103897, 2020.
- [10] Joyce A Martin, Brady E Hamilton, Paul D Sutton, Stephanie J Ventura, Fay Menacker, Sharon Kirmeyer, and Martha L Munson. Births: final data for 2005. *National vital statistics reports*, 56(6):1–103, 2007.
- [11] Marian F MacDorman, William M Callaghan, TJ Mathews, Donna L Hoyert, and Kenneth D Kochanek. Trends in preterm-related infant mortality by race and ethnicity, united states, 1999–2004. *International Journal of Health Services*, 37(4):635–641, 2007.
- [12] John Bechhoefer. *Control theory for physicists*. Cambridge University Press, 2021.